Plant Physiol. (1997) 113: 469–477

Reduction of Ribulose-1,5-Bisphosphate Carboxylase/Oxygenase by Antisense RNA in the C_4 Plant *Flaveria bidentis* Leads to Reduced Assimilation Rates and Increased Carbon Isotope Discrimination

Susanne von Caemmerer*, Anthony Millgate, Graham D. Farquhar, and Robert T. Furbank

Research School of Biological Sciences, Australian National University, GPO Box 475, Canberra 2601, Australia (S.v.C., A.M., G.D.F.); Commonwealth Scientific and Industrial Research Organization, Divison of Plant Industry, GPO Box 1600, Canberra 2601, Australia (R.T.F.); and Co-Operative Research Centre for Plant Science, GPO Box 475, Canberra 2601, Australia (G.D.F., R.T.F.)

Transgenic *Flaveria bidentis* (a C_4 species) plants with an antisense gene directed against the mRNA of ribulose-1,5-bisphosphate carboxylase/oxygenase (Rubisco) were used to examine the relationship between the CO_2 assimilation rate, Rubisco content, and carbon isotope discrimination. Reduction in the amount of Rubisco in the transgenic plants resulted in reduced CO_2 assimilation rates and increased carbon isotope discrimination of leaf dry matter. The H_2O exchange was similar in transgenic and wild-type plants, resulting in higher ratios of intercellular to ambient CO_2 partial pressures. Carbon isotope discrimination was measured concurrently with CO_2 and H_2O exchange on leaves of the control plants and T_1 progeny with a 40% reduction in Rubisco. From the theory of carbon isotope discrimination in the C_4 species, we conclude that the reduction in the Rubisco content in the transgenic plants has led to an increase in bundle-sheath CO_2 concentration and CO_2 leakage from the bundle sheath; however, some down-regulation of the C_4 cycle also occurred.

The C_4 photosynthetic pathway requires the coordinated functioning of mesophyll and bundle-sheath cells within a leaf. Reactions of the C_4 cycle concentrate CO_2 in the bundle-sheath cells for assimilation by Rubisco (Hatch, 1987). This enhances Rubisco carboxylation while at the same time inhibiting Rubisco oxygenation, thus reducing the amount of photorespiration. The energy cost of this CO_2-concentrating mechanism is 2 mol of ATP per regeneration of 1 mol of the primary CO_2 acceptor PEP, and any CO_2 that leaks from the bundle sheath rather than being fixed by Rubisco reduces the efficiency of the concentrating mechanism (Hatch, 1987). The compartmentation of the photosynthetic process between mesophyll and bundle-sheath cells has complicated the study of C_4 photosynthesis, and the biophysical characterization of the CO_2-concentrating function of C_4 photosynthesis has been experimentally difficult. Many of the parameters, such as bundle-sheath CO_2 concentration or the leakiness (ϕ) of the bundle sheath (defined as the fraction of CO_2 generated by C_4 acid decarboxylation that subsequently leaks out), cannot be measured directly, although estimates ranging from 8 to 40% have been made in various ways (Hatch and Osmond, 1976; Farquhar, 1983; Furbank and Hatch, 1987; Bowmann et al., 1989; Jenkins et al., 1989; Henderson et al., 1992; Hatch et al., 1995). For example, theoretical treatments of carbon isotope discrimination (Δ) that occur during C_4 photosynthesis have shown that leakage of CO_2 from the bundle sheath is one of the major factors influencing Δ during CO_2 uptake in C_4 species (O'Leary, 1981; Peisker, 1982; Deleens et al., 1983; Farquhar, 1983). In particular, Farquhar (1983) developed a simple equation that relates Δ to the ratio of intercellular to ambient CO_2, p_i/p_a, and ϕ.

ϕ depends on the physical conductance of the bundle-sheath cell wall and on the balance of the biochemical capacities of the C_4 and C_3 cycles. To date, the only method available to test models of carbon isotope discrimination and leakiness has been to examine plants with interspecific differences in the carbon isotope ratio. Such comparisons are difficult because both the amount of the C_4 and C_3 cycle enzymes may be different, and bundle-sheath cell conductance may vary across widely disparate species. Recently it has become possible to perturb the balance between the C_3 and C_4 cycles in a single species with an otherwise uniform genetic background using recombinant DNA technology. The C_4 dicot *Flaveria bidentis* has been transformed with an antisense RNA construct targeted to the nucleus-encoded gene for the small subunit of Rubisco (Chitty et al., 1994; Furbank et al., 1996). These antisense transformants had reduced amounts of Rubisco, but there was no apparent effect from transformation with the gene construct on the maximum extractable activity of other photosynthetic enzymes. If in vitro-extracted enzyme activities reflect in vivo capacities, one might expect leakiness to have increased in the transformants, resulting in greater carbon isotope discrimination. Here we used the T_1 progeny of three trans-

* Corresponding author; e-mail susanne@rsbs-central.anu.edu.au; fax 61–6–2495075.

Abbreviations: p_a, ambient CO_2 partial pressure; ϕ, leakiness; p_i, intercellular CO_2 partial pressure; RuBP, ribulose-1,5-bisphosphate.

formed lines to examine the effect of a reduction of Rubisco on CO_2 assimilation, carbon isotope discrimination, and ϕ.

MATERIALS AND METHODS

Plant Culture

Flaveria bidentis (L.) Kuntze was previously transformed with an antisense RNA construct targeted to the nucleus-encoded gene for the small subunit of Rubisco (Chitty et al., 1994; Furbank et al., 1996). Primary transformants were allowed to self-fertilize and T_1 seed of the three primary transformants 141–1 (one insert), 136–6, and 136–13 (four inserts) were sown in sterilized garden soil together with T_1 seed of control transformants (transformed with a T-DNA carrying the gene for GUS). Seedlings were transplanted into 8-cm pots and later transferred into 20-cm pots. Plants were either grown in a naturally lit greenhouse (the progeny of 141–1 and 136–6 from July to September 1995, the progeny of 136–13 in February 1996) or in a growth cabinet (28/20°C day/night temperature, 700 μmol quanta m^{-2} s^{-1}, and a 16-h photoperiod). Plants were given a complete nutrient solution containing 12 mM nitrate (Hewitt and Smith, 1975) three times a week.

Gas-Exchange Measurements and Experimental Protocol

The youngest, fully expanded leaves of transgenic and control plants were used for gas-exchange measurements. Samples were taken from the same leaves immediately after these measurements and stored at −80°C for later analysis of enzyme activity. The opposite leaf was oven-dried at 60°C for later analysis of dry-matter carbon isotope composition. Gas-exchange measurements were made with an open gas exchange system (model 6400, Li-Cor, Lincoln, NE) with illumination provided by a red light emitting diodes light source (660–675 nm, Li-Cor), except when gas-exchange measurements were made concurrently with measurements of carbon isotope discrimination. In that case gas-exchange measurements were made as described by von Caemmerer and Evans (1991).

Carbon Isotope Measurements

Carbon isotope discrimination, Δ, was measured concurrently with gas exchange by collecting the CO_2 leaving the leaf chamber with and without a leaf enclosed (von Caemmerer and Evans, 1991). The CO_2 collected was analyzed for its ^{13}C:^{12}C ratio with a dual-inlet-ratio mass spectrometer (SIRA24, VG Isogas, Middlewich, UK). The carbon isotope composition of CO_2 in the gas-exchange system was −24.6‰ with respect to the standard Pee Dee Belemnite. Measurements made on gas samples collected from the empty chamber had a SD of 0.031‰. CO_2 was collected after the gas exchange of leaves had reached steady-state values at 2000 μmol quanta m^{-2} s^{-1}, a leaf temperature of 25°C, and an ambient CO_2 concentration of 350 μbar.

The carbon isotope discrimination during gas exchange of leaves, Δ, was calculated from the difference in the carbon isotope compositions of the air leaving the chamber with (δ_o) and without (δ_e) a leaf enclosed (Evans et al., 1986; von Caemmerer and Evans, 1991):

$$\Delta = \frac{\xi(\delta_o - \delta_e)}{1 + \delta_o - \xi(\delta_o - \delta_e)}, \quad (1)$$

where $\xi = p_e/(p_e - p_o)$, and p_e and p_o are the CO_2 partial pressures at a standard humidity of the air entering and leaving the chamber, respectively. The precision of the measurement of Δ to a large degree is determined by ξ, which varied between 4 and 8.

Carbon isotope composition of leaf dry matter was measured on finely ground leaf dry matter and calculated from the carbon isotope composition, with respect to the standard Pee Dee Belemnite of the dry matter (δ_p) and the greenhouse air ($\delta_a = -8.75$‰) as

$$\Delta = (\delta_a - \delta_p)/(1 + \delta_p) \quad (2)$$

(Henderson et al., 1992; Farquhar et al., 1989).

Calculation of ϕ

We used the equations derived by Farquhar (1983) to estimate ϕ from concurrent measurements of Δ and the ratio of intercellular and ambient partial pressure of CO_2 (p_i/p_a):

$$\Delta = a + (b_4 + \phi(b_3 - s) - a)p_i/p_i, \quad (3)$$

where a (4.4‰) is the fractionation during diffusion of CO_2 in air (Farquhar et al., 1989), b_4 (−5.7‰) is the combined fractionation of PEP carboxylation (2.2‰) and the preceding isotopic equilibrium during dissolution of CO_2 and conversion to bicarbonate, b_3 (30‰) is the fractionation by Rubisco, and s (1.8‰) is the fractionation during leakage, which we assumed to be equal to the fractionation occurring as CO_2 dissolves in the bundle sheath and diffuses back to the mesophyll. Equation 3 can be rearranged as an explicit expression for ϕ:

$$\phi = \frac{\Delta - a + (a - b_4)p_i/p_a}{(b_3 - s)p_i/p_a}. \quad (4)$$

Biochemical Assays

Following gas-exchange measurements, leaf discs (0.5 cm^2) were collected and frozen in liquid nitrogen and stored at −80°C for subsequent analysis.

Rubisco and PEP carboxylase activities were measured by the incorporation of $H^{14}CO_3^-$ into acid-stable products at 25°C. Leaf discs were extracted in 500 μL of buffer containing 50 mM Hepes-KOH, pH 7.1, 5 mM $MgCl_2$, 1 mM sodium EDTA, 15 mM $NaHCO_3$, 10 mM DTT, 1 mM PMSF, and 1% polyvinylpolypyrrolidone at room temperature. Rubisco activity was assayed on 25 μL of extract after a 10-min incubation at 25°C in 225 μL of assay buffer (50 mM *N*-[2 hydroxyethyl]piperazine-*N*′-[3 prapane sulfonic acid], pH 8.2, 20 mM $MgCl_2$, 0.25 mM sodium EDTA, and 20 mM $NaH^{14}CO_3^-$ [960 TBq mol^{-1}]). The assays were initiated with 5 μL of 20 mM RuBP and terminated after 1 min with 125 μL of concentrated formic acid. PEP carboxylase

activity was measured immediately after extraction in 225 μL of buffer (50 mM Bicine, pH 8.2, 10 mM $MgCl_2$, 10 mM $NaH^{14}CO_3^-$ [960 TBq mol^{-1}], 10 mM DTT, 5 mM Glc-6-P, 0.2 mM NADH, and 3 units of malate dehydrogenase) and the assay was initiated with 15 μL of 100 mM PEP and terminated after 1 min with 125 μL of concentrated formic acid. All assays were run in triplicate.

Rubisco content was determined from the [^{14}C]2′-carboxy-D-arabinitol-1,5-bisphosphate binding assay (Butz and Sharkey, 1989; Mate et al., 1993) and soluble protein was quantified using the Coomassie Plus reagent (Pierce) on the same extracts.

RESULTS

Figures 1 and 2 summarize the results obtained for the greenhouse-grown plants. The lowest Rubisco content observed among the T_1 progeny of primary transformant 141–1 was approximately 40% of the controls. The T_1 progeny of primary transformant 136–6 and 136–13 spanned a greater range, with the lowest Rubisco content being approximately 10% of the control.

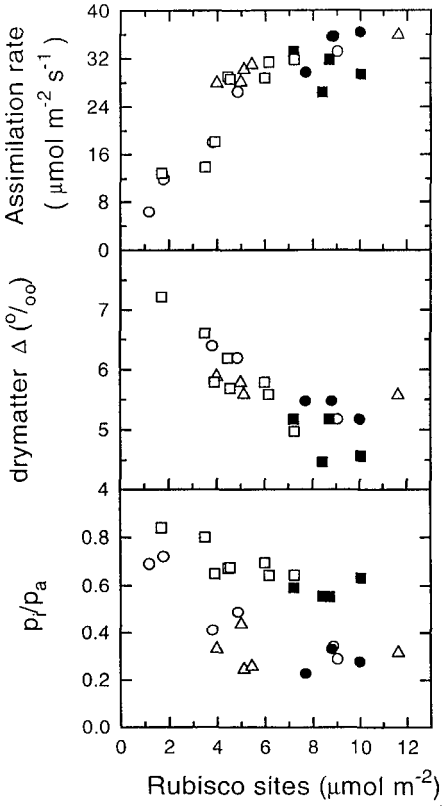

Figure 1. CO_2 assimilation rate, dry matter carbon isotope discrimination, and the ratio of intercellular to ambient CO_2 (p_i/p_a) as a function of Rubisco site content. Measurements were made on the youngest, fully expanded leaves of control plants (●, ■) and plants of the T_1 progeny of primary transformants 141–1 (△), 136–6 (○), and 136–13 (□) that were grown in the glasshouse. The progeny of 136–13 were grown at a later date and controls marked with a ■ were grown at the same time. Gas-exchange conditions were set at an ambient CO_2 concentration of 350 μbar, an irradiance of 2000 μmol quanta m^{-2} s^{-1}, a leaf-to-air vapor difference of 10 mbar, and a leaf temperature of 25°C.

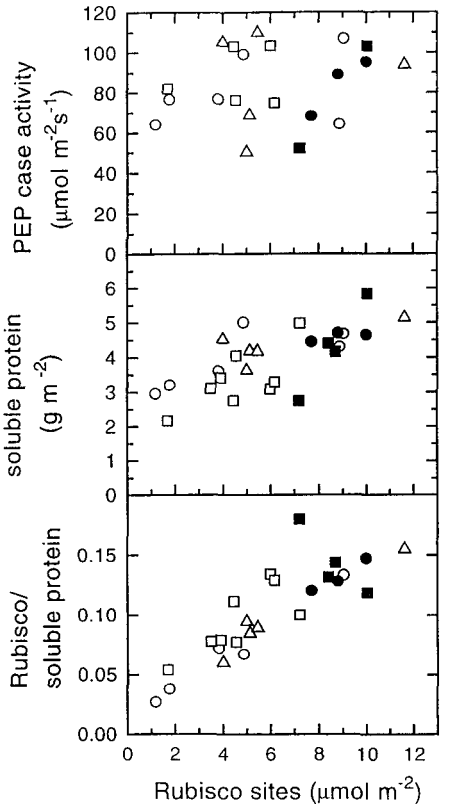

Figure 2. PEP carboxylase activity, soluble protein content, and the ratio of Rubisco to soluble protein as a function of Rubisco site content. Measurements were made on the same leaves on which gas exchange was measured, and symbols are as described in Figure 1.

There was a strong correlation between the CO_2 assimilation rate (measured at ambient CO_2 of 350 μbar and 2000 μmol quanta m^{-2} s^{-1}) and the Rubisco content of leaves (Fig. 1) (Furbank et al., 1996). The decrease in the CO_2 assimilation rate was accompanied by an increase in p_i/p_a, suggesting that stomatal conductance had not been reduced to the same extent as the CO_2 assimilation rate. The ratio of p_i/p_a was higher in the measurements made in February, which may have been caused by growth conditions in the greenhouse. The reduction in Rubisco also led to an increase in leaf dry matter carbon isotope discrimination (Fig. 1).

There was no significant effect of the transformation with the antisense gene on PEP carboxylase activity in the greenhouse-grown plants (Fig. 2) There was a slight reduction in soluble protein, however, and Rubisco declined from forming 15% of the soluble protein in the controls to only 3% in plants with the least amount of Rubisco.

Among the growth-cabinet-grown plants, no individuals with very low Rubisco contents were isolated in the T_1 progeny of 136–6. The T_1 progeny of 141–1 showed a spread of Rubisco content similar to that seen with the greenhouse-grown plants. Two controls and three progeny of the primary transformant 141–1, with the lowest Rubisco contents, were chosen for detailed gas-exchange analysis

and measurements of carbon isotope discrimination during gas exchange. The biochemical details of the measured leaves are shown in Table I. All three transformants had similar CO_2 assimilation rates. The average Rubisco content was 40% of the wild type; however, the PEP carboxylase activity was greater in the transformants than in the controls. (Table I).

Figure 3 shows the CO_2 assimilation rate as a function of intercellular CO_2 concentration for the leaves that were used for concurrent measurements of CO_2 uptake and carbon isotope discrimination. The reduction in Rubisco content led to a reduction in the CO_2-saturated rate of CO_2 assimilation, whereas there was no difference in the initial slope of the CO_2 response curves for transformants or control plants.

Measurements of carbon isotope discrimination during CO_2 uptake were made at an ambient CO_2 of 350 μbar, which, under these conditions, was sufficient to saturate the CO_2 assimilation rates. In Figure 4 short-term measurements of carbon isotope discrimination (Δ) are plotted against p_i/p_a for control and antisense plants. The lines shown describe the theoretical relationship between Δ and p_i/p_a (Farquhar, 1983) (see Eq. 3 in "Materials and Methods") for the two mean values of ϕ calculated from the data. Since antisense plants had greater Δ values and greater ratios of p_i/p_a, the carbon isotope discrimination theory predicts a greater ϕ for these plants. Measurements of carbon isotope composition of dry matter were not made on these leaves, because the carbon isotope ratio of growth-cabinet air fluctuates too widely to obtain meaningful results.

Quantum yield measurements were also made on five leaves of control and four leaves of antisense plants with the Li-Cor 6400 gas-exchange system at 25°C with an ambient CO_2 partial pressure of 350 μbar and a red light emitting diode light source. Measurements were made between 80 and 180 μmol quanta m^{-2} s^{-1}. The mean quantum yield of the control leaves was 0.0403 ± 0.003 and 0.038 ± 0.003 (CO_2 per incident photon) for the antisense transformants; the 5.2% difference was not significant. There was no significant difference in the chlorophyll content between controls and transformants and the mean chlorophyll content was 650 μmol m^{-2}. Assuming 80% absorptance in both cases, the observed quantum yields were 0.053 and 0.047, respectively, on an absorbed light basis.

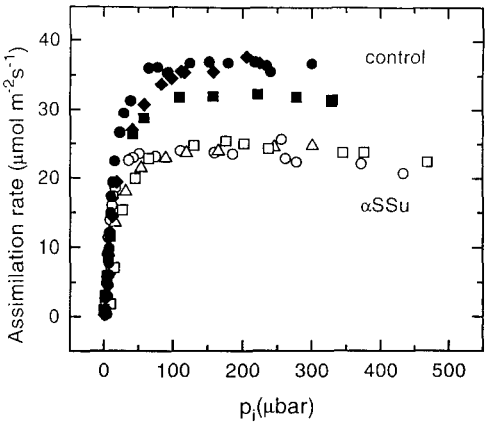

Figure 3. CO_2 response curve of the CO_2 assimilation rate for the youngest, fully expanded leaves of control (C6 [■], C11a [●], and C11b [◆]) and antisense *F. bidentis* (141–1,2 [○], 141–1,4 [□], and 141–1,15 [△]) plants grown in a growth cabinet. Gas-exchange conditions are as described in Figure 1 except that CO_2 was varied. Biochemical characteristics are given in Table I. The same leaves or the opposite leaf were used for short-term measurements of carbon isotope discrimination (see Fig. 4).

DISCUSSION

Antisense Effect on Leaf Biochemistry and Photosynthesis

Among the T_1 progeny of the primary transformants 141–1, 136–6, and 136–13, we identified several transformants with reduced amounts of Rubisco (Fig. 1; Table I). Consistent with the results obtained on the primary transformants (Furbank et al., 1996), the antisense gene construct did not reduce PEP carboxylase activity, whereas the Rubisco content decreased as a fraction of the soluble protein (Fig. 2; Table I) (Furbank et al., 1996). Under our growth conditions Rubisco constituted approximately 12 to 15% of the leaf soluble protein in the *F. bidentis* control plants, one-half of what is normally observed in C_3 plants (e.g. Evans et al., 1994). This is consistent with previous observations that the C_4 species use nitrogen more efficiently than

Table I. *Biochemical characteristics of control and Rubisco antisense (αSSu) F. bidentis leaves on which short-term measurements of carbon isotope discrimination were made*

Plant No.	Assimilation Rate	Rubisco Sites	Rubisco k_{cat}	PEP Carboxylase Activity	PEP Carboxylase to Rubisco Activity Ratio	Soluble Protein	Ratio of Rubisco to Soluble Protein
	$\mu mol\ m^{-2}\ s^{-1}$	$\mu mol\ m^{-2}$	s^{-1}	$\mu mol\ m^{-2}\ s^{-1}$		$g\ m^{-2}$	
Controls							
C6	31.8	9.2	3.2	166	5.6	6.7	0.09
C11a	36.4	10.5	3.4	126	3.5	5.5	0.13
C11b	37.7	9.5	2.6	135	5.5	5.7	0.11
αSSu							
(141, 1)2	22.8	2.9	3.8	215	19.0	6.4	0.03
(141, 1)4	24.5	5.6	3.8	205	9.8	6.73	0.06
(141, 1)15	23.7	3.3	3.5	211	18.1	6.35	0.04

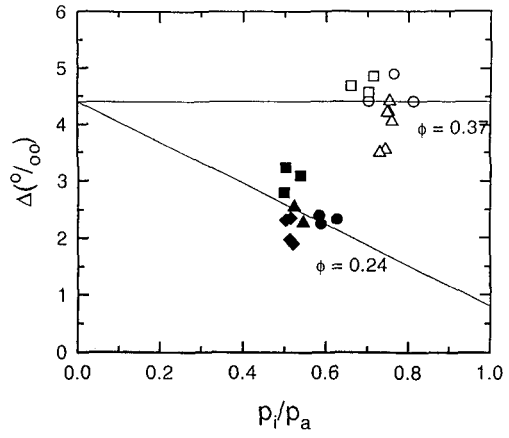

Figure 4. Carbon isotope discrimination (Δ) as a function of intercellular to ambient partial pressure of CO_2 (p_i/p_a) in control (closed symbols) and Rubisco antisense *Flaveria* plants (open symbols) grown in growth cabinets. Individual symbols are replicate measurements on single leaves and symbols are defined in Figure 3. Carbon isotope measurements were made concurrently with gas exchange and conditions were as described in Figure 1. The lines depict the theoretically predicted relationship where $\Delta = 4.4 + (28.8\phi - 10.1)\ p_i/p_a$.

the C_3 species, since Rubisco can operate near its maximal activity (Brown, 1978; Usuda, 1984; Sage et al., 1987).

CO_2 Response Curves

There was a close correlation between the CO_2 assimilation rate and the Rubisco content for measurements that were made at a high irradiance and 350 μbar of CO_2, demonstrating that Rubisco is of equal importance in both the C_4 and C_3 species in determining photosynthetic rate (Fig. 1) (Hudson et al., 1992; Furbank et al., 1996). However, the difference in the photosynthetic mechanism is apparent in the contrasting effect that a reduction of Rubisco has on the CO_2 response of CO_2 assimilation (Fig. 3). In C_3 species Rubisco activity determines the initial slope of the CO_2 response curve, and saturation at higher CO_2 is determined by the capacity of the RuBP regeneration capacity (von Caemmerer and Farquhar, 1981; Hudson et al., 1992). Figure 3 shows that in *F. bidentis* a reduction in Rubisco has led to a reduction in the CO_2-saturated rate of CO_2 assimilation but has not affected the initial slope of the response curve. These results are in agreement with the models of C_4 photosynthesis, which predicted that the initial slope of these curves is determined by PEP carboxylase activity, whereas the saturated rate can be determined by the maximal Rubisco activity or the capacities of RuBP or PEP regeneration (Berry and Farquhar, 1978, Collatz et al., 1992). Thus, the CO_2 response curves in Figure 3 provide in vivo evidence that the antisense construct has created an imbalance between the C_4 and C_3 cycles. It is notable that in our previous study (Furbank et al., 1996) we observed the effects of the Rubisco antisense construct on the initial slope of the CO_2 response curve. This may have been because the T_0 material examined earlier exhibited a more severe phenotype than the moderately affected plants shown in Figure 3.

Correlation between CO_2 Assimilation Rate and Rubisco Content

It appears that there is enough Rubisco available to support the maximal photosynthetic rate in the control plants. In vitro we measured the catalytic activity of 3.4 s^{-1} per Rubisco site (Table I), and the CO_2 assimilation rates of control plants are, thus, similar to their maximal Rubisco activities. This is what one would expect if (at high bundle-sheath CO_2 concentrations) Rubisco operates close to its maximal activity. Good correlations between the CO_2 assimilation rate and maximal Rubisco activity have been demonstrated previously, e.g. when variation in Rubisco activity was the result of different leaf ages or different nitrogen nutrition (Usuda, 1984; Hunt et al., 1985; Sage et al., 1987). Frequently, however, the low maximal activities measured for pyruvate Pi dikinase have been used to infer its possible role in limiting CO_2 fixation at a high irradiance (Sugiyama and Hirayama, 1983; Usuda, 1984; Usuda et al., 1984). The slight saturation of the CO_2 assimilation rate at high Rubisco contents could be interpreted in this way (Fig. 1).

However, it is important to realize that a reduction in Rubisco content via the antisense construct may have quite a different effect on CO_2 assimilation, bundle-sheath CO_2 concentration, and ϕ than a reduction of the Rubisco content resulting from leaf senescence or nitrogen nutrition. These differences are illustrated in Figure 5 with the use of a model of C_4 photosynthesis (Berry and Farquhar, 1978) (see "Appendix"). We assume that in the antisense plants Rubisco is reduced, with no change in bundle-sheath conductance or rate of PEP carboxylation (Fig. 5, solid line). This leads to a nonlinear decrease in the CO_2 assimilation rate with a decrease in Rubisco, because we chose a $K_m(CO_2)$ of 1300 μbar for the C_4 Rubisco at 21% O_2 (Jordan and Ogren, 1991) (see "Appendix"). This allows for a slight increase in Rubisco carboxylations with the increase in bundle-sheath CO_2. Both bundle-sheath CO_2 and ϕ are predicted to increase with a decrease in Rubisco content with antisense plants (Fig. 5, solid line).

With leaf aging or differences in nitrogen nutrition, PEP carboxylase activity and other enzyme activities and presumably bundle-sheath conductance may covary with Rubisco activity. The dashed lines in Figure 5 mimic this case; bundle-sheath CO_2 concentration and ϕ are constant with a decrease in Rubisco and there is a linear relationship between Rubisco and the CO_2 assimilation rate, as has been observed (Usuda, 1984). The absolute values of the CO_2 assimilation rate, bundle-sheath CO_2 concentration, and ϕ shown in Figure 5 are, of course, strongly dependent on the choice of parameters, such as bundle-sheath conductance to CO_2 and PEP carboxylase activity. The bundle-sheath conductance that we chose is similar to that measured by Brown and Byrd (1993).

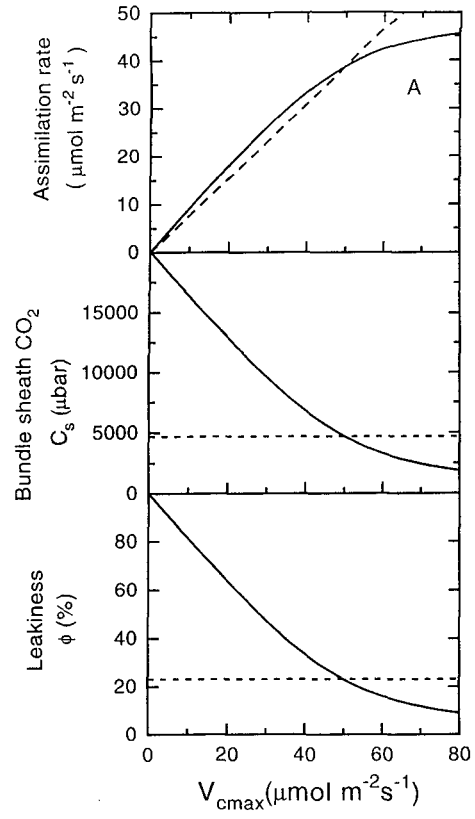

Figure 5. Modeled response of CO_2 assimilation rate, bundle-sheath CO_2 concentration (C_s), and ϕ to changes in maximal Rubisco activity (V_{cmax}) at a constant maximal PEP carboxylase activity (V_{pmax}) of 90 μmol m^{-2} s^{-1} and bundle-sheath conductance of 2.5 mmol m^{-2} s^{-1} and an intercellular CO_2 concentration of 100 μbar (solid lines), or at a constant ratio V_{pmax}/V_{cmax} of 1.8 and a bundle-sheath conductance of 50 V_{cmax} (dashed lines). The model equations and kinetic constants used are given in the "Appendix" and Table II.

Antisense Effects on ϕ and Carbon Isotope Discrimination

Carbon Isotope Discrimination Measured Concurrently with CO_2 Exchange

Theoretical treatments of carbon isotope discrimination occurring during C_4 photosynthesis have shown that leakage of CO_2 from the bundle sheath is one of the major factors influencing carbon isotope discrimination during CO_2 uptake in the C_4 species (O'Leary, 1981; Peisker, 1982; Deleens et al., 1983; Farquhar, 1983). Farquhar (1983) developed simple equations that related Δ to the ratio of p_i/p_a and ϕ (see "Materials and Methods," Eqs. 3 and 4). The lines in Figure 4 give the theoretical dependence of Δ on p_i/p_a at different values of ϕ. The carbon isotope discrimination and the calculated ϕ of 24% of the control *F. bidentis* are similar to previous measurements on *F. bidentis* (Henderson et al., 1992; Hatch et al., 1995). Carbon isotope discrimination and the ratio of p_i/p_a are greater in the transgenic plants, leading to a greater calculated ϕ of 37%. This suggests that the reduction in Rubisco has led to an increase in bundle-sheath CO_2 concentration and, as a consequence, to an increased rate of CO_2 leakage out of the bundle sheath. This conclusion is also supported by measurements of carbon isotope discrimination of leaf dry matter in greenhouse-grown plants (Fig. 1).

If the lower CO_2 assimilation rate of the transformants (Fig. 1; Table I) was caused solely by an increase in the bundle-sheath leak rate, we should have observed a greater increase in ϕ for the observed incremental reduction in CO_2 assimilation rate and Rubisco content than we predict from the carbon isotope analysis. This, of course, assumes that no other changes in metabolic regulation occurred. Henderson et al. (1992) estimated ϕ under a wide variety of conditions including short-term variations in irradiance, ambient CO_2 concentration, and leaf temperature and found very little variation in ϕ, suggestive of some coregulation between the C_4 and C_3 cycles. This conclusion was reached earlier by Furbank and Leegood (1984) from evidence of close coupling between the metabolite pools of 3-phosphoglycerate and PEP in maize leaves. It is possible that the reduction in the Rubisco content in our experimental material also reduced the regeneration rate of PEP to some extent, minimizing the amount of overcycling of the C_4 cycle (see Furbank et al., 1996).

Dry Matter Carbon Isotope Discrimination

The carbon isotope composition of leaf dry matter gives an integrated value of carbon isotope discrimination over the lifetime of a leaf, which includes temporal variations in stomatal conductances, ϕ, and possible postphotosynthetic discriminations. Consequently, the data cannot be used for a quantitative analysis of ϕ. Nevertheless, the dry matter Δ of the transformants measured here increased with decreasing Rubisco content (Fig. 1). Since the spot measurement of gas exchange shows that p_i/p_a also increased, the data indicate a further increase in ϕ in transformants with the lower Rubisco levels than in the progeny of primary transformants 141–1 (Fig. 1). The mean carbon isotope discrimination of leaf dry matter for control leaves was 5.27‰, which is 2.5‰ greater than the mean carbon isotope discrimination of 2.8‰ measured during gas exchange. These results and differences are similar to the previous comparisons made by Henderson et al. (1992). Very few comparisons have been made between dry matter Δ values and measurements made during gas exchange. The difference between dry matter Δ and that measured during gas exchange is perhaps to some extent related to inaccurate measurements of the carbon isotope composition of the greenhouse air (Eq. 2), or it could be an indication that further carbon isotope discrimination subsequent to that occurring during CO_2 fixation has taken place (Henderson et al., 1992).

Quantum Yields and ϕ

The quantum yield of CO_2 assimilation was measured on the same or similar plants as those used for the measurements of carbon isotope discrimination during gas exchange. There were no significant differences in the quantum yields between the control plants and transformants, although the carbon isotope discrimination indicated a dif-

ference of ϕ at high irradiance. This was somewhat surprising, since the wide range of quantum yield values reported for C_4 plants is often attributed to variations in leakiness and overcycling (Ehleringer and Pearcy, 1982; Farquhar, 1983; Furbank et al., 1990). However, this observation is consistent with the notion that a reduction in Rubisco in the bundle sheath affects CO_2 assimilation rates only at a high irradiance (Furbank et al., 1996). Because of the uncertainty about the level of Q-cycle activity, a mechanism for proton translocation through the cytochrome *b/f* complex, it is difficult to infer precisely what changes in the quantum yield should occur (Furbank et al., 1990). If we assume that 1 mol of quanta is required for 1 mol of protons, 3 mol of protons are needed for the generation of 1 mol of ATP, and, in turn, 2 mol of ATP is required for the regeneration of 1 mol of PEP in the C_4 cycle and 3 mol of ATP is required for the regeneration of 1 mol of RuBP in the bundle sheath, then $(1 - \phi)$ mol CO_2 fixed requires $6 + 9(1 - \phi)$ mol quanta and the quantum yield is $(1 - \phi)/(15 - 9\phi)$. The relationship between quantum yield and ϕ is nonlinear, and our measured ϕ of 24 and 37% correspond to only a 8% difference in the quantum yield. Given the uncertainties of quantum yield measurements and their interpretations, they may be of limited use as sensitive indicators of ϕ.

APPENDIX

In this appendix we derive the key equations used in Figure 5 to calculate the CO_2 assimilation rate (A) bundle-sheath CO_2 partial pressure (C_s), and ϕ from Rubisco and PEP carboxylase activities and bundle-sheath conductance (g_s). The equations given are based on the C_4 model by Berry and Farquhar (1978) (but see also Collatz et al., 1992).

The CO_2 assimilation rate of C_4 photosynthesis can be described by two simple equations. Since ultimately all CO_2 is fixed by Rubisco in the bundle sheath, the net rate of CO_2 assimilation (A) is

$$A = V_c - 0.5V_o - R_d, \tag{A1}$$

where V_c and V_o are the rates of Rubisco carboxylation and oxygenation and R_d is the rate of mitochondrial respiration not associated with photorespiration. Mitochondrial respiration may occur in the mesophyll as well as in the bundle sheath, and because CO_2 released in the bundle sheath may be more readily refixed by Rubisco, we also describe R_d by its mesophyll and bundle-sheath components

$$R_d = R_m + R_s. \tag{A2}$$

The bundle-sheath compartment is a semiclosed system and is dependent for its supply of CO_2 on the decarboxylation of C_4 acids from the mesophyll cells. From the viewpoint of the mesophyll cells, the CO_2 assimilation rate can be given by

$$A = V_p - L - R_m, \tag{A3}$$

where V_p is the rate of PEP carboxylation (we assume it to be equal to the rate of C_4 acid decarboxylation), R_m is the the mitochondrial respiration in the mesophyll, and L is the rate of CO_2 leakage across the bundle sheath. The leakage (L), in turn, is given by

$$L = g_s(C_s - C_m), \tag{A4}$$

where g_s is the physical conductance of the bundle sheath to CO_2 and C_s and C_m are the bundle-sheath and mesophyll CO_2 partial pressures. ϕ then defines leakage as a fraction of the rate of PEP carboxylation

$$\phi = L/V_p. \tag{A5}$$

We assume that at a high irradiance the maximal activities of enzymes such as PEP carboxylase, Rubisco, and perhaps pyruvate Pi dikinase limit the rate of CO_2 fixation rather than the light-dependent capacities for the regeneration of RuBP and PEP, which are not considered here.

Rubisco carboxylations can then be described by the RuBP saturated rate

$$V_c = \frac{C_s V_{cmax}}{C_s + K_c(1 + O_s/K_o)}, \tag{A6}$$

where V_{cmax} is the maximum carboxylation rate, K_c and K_o are the Michaelis-Menten constants for CO_2 and O_2, and O_s is the O_2 concentration in the bundle sheath. Following the oxygenation of 1 mol of RuBP, 0.5 mol of CO_2 is evolved in the photorespiratory pathway, and Farquhar et al. (1980) showed that the ratio of oxygenation to carboxylation can be expressed as

$$V_o/V_c \approx 2\Gamma_*/C_s, \tag{A7}$$

where Γ_* is the CO_2 compensation point in a C_3 plant in the absence of other mitochondrial respiration, and furthermore

$$\Gamma_* = [0.5V_{omax}K_c/(V_{cmax}K_o)]O_s = \gamma_* O_s, \tag{A8}$$

where V_{omax} is the maximal oxygenase activity.

From the above it can be shown that

$$A = \frac{(C_s - \gamma_* O_s)V_{cmax}}{C_s + K_c(1 + O_s/K_o)} - R_d. \tag{A9}$$

PSII activity and the amount of O_2 evolution occurring in the bundle sheath varies among the C_4 species, with NADP-malic enzyme species such as *Zea mays* and *Sorghum bicolor* having little to none. Because the bundle sheath is fairly gas-tight, this has implications for the steady-state O_2 concentration in the bundle sheath (Raven, 1977). *F. bidentis*, an NADP-malic enzyme species, may have little O_2 evolution in the bundle sheath, so that O_2 concentrations there are similar to that in the mesophyll, but for completeness we give the more general expression for the bundle-sheath O_2 concentration. Following Berry and Farquhar (1978) we assume that the net O_2 evolution (E_o) in the bundle-sheath cells equals its leakage (L_o) out of the bundle sheath, that is

$$E_o = L_o = g_o(O_s - O_m), \tag{A10}$$

where O_m is the mesophyll O_2 concentration. The conductance to leakage of O_2 across the bundle sheath (g_o) is

related to the conductance to CO_2 by way of the ratio of diffusivities and solubilities by

$$g_o = g_s(D_{O2}S_{O2}/D_{CO2}S_{CO2}), \quad \text{(A11)}$$

where D_{O2} and D_{CO2} are the diffusivities for O_2 and CO_2 in water, respectively, and S_{O2} and S_{CO2} are the respective Henry constants such that

$$g_o = 0.047g_s \quad \text{(A12)}$$

at 25°C (Farquhar, 1983). If $E_o = \alpha A$, where α denotes the fraction of O_2 evolution occurring in the bundle sheath and $(0 < \alpha < 1)$, then

$$O_s = \frac{\alpha A}{0.047g_s} + O_m. \quad \text{(A13)}$$

That is, when no oxygen evolution is occurring in the bundle sheath ($\alpha = 0$), $O_s = O_m$, which is what has been assumed in Figure 5.

We write the rate of PEP carboxylation as

$$V_p = \frac{C_m V_{pmax}}{C_m + K_p}, \quad \text{(A14)}$$

where V_{pmax} is the maximal activity of PEP carboxylase and K_p is the Michaelis-Menten constant for CO_2. If enzymes such as pyruvate Pi dikinase were to limit the rate of PEP regeneration, one could set V_p = constant.

To obtain an overall rate equation for CO_2 assimilation as a function of the mesophyll CO_2 and O_2 partial pressures (C_m and O_m, respectively), one can use either of the following expressions for bundle-sheath CO_2 concentration:

$$C_s = \frac{\gamma_* O_s + K_c(1 + O_s/K_o)([A + R_d]/V_{cmax})}{1 - (A + R_d)/V_{cmax}}, \quad \text{(A15)}$$

which is derived from Equation A9 or

$$C_s = C_m + \frac{Vp - A - R_m}{g_s}, \quad \text{(A16)}$$

which is derived from Equations A3 and A4.

Combining Equations A16 and A13 with Equations A9 or A16, and Equation A13 with Equations A3 and A4, results in a quadratic expression of the form

$$aA^2 + bA + c = 0, \quad \text{(A17)}$$

where

$$A = (-b + \sqrt{b^2 - 4ac})/(2a) \quad \text{(A18)}$$

and

$$a = 1 - \frac{\alpha}{0.047}\frac{K_c}{K_o} \quad \text{(A19)}$$

$$b = -\{(V_p - R_m + g_sC_m) + (V_{cmax} - R_d) + g_s(K_c(1 + O_m/K_o)) + \alpha/0.047(\gamma_* V_{cmax} + R_d K_c/K_o)\} \quad \text{(A20)}$$

$$c = (V_p - R_m + g_sC_m)(V_{cmax} - R_d) - (V_{cmax}g_s\gamma_* O_m + R_d g_s K_c[1 + O_m/K_o]). \quad \text{(A21)}$$

Table II. *Parameters used in the model*

Symbol		Definition
V_{cmax}	60 μmol m^{-2} s^{-1} or variable	Maximum Rubisco activity
K_c	1015 μbar[a]	Michaelis constant of Rubisco for CO_2
K_o	675 mbar[a]	Michaelis constant of Rubisco for O_2
γ_*	0.00035[a]	$0.5/(S_{c/o})$, where $S_{c/o}$ denotes Rubisco specificity
V_{pmax}	120 μmol m^{-2} s^{-1} or variable	Maximum PEP carboxylase activity
K_p	80 μbar[b]	Michaelis constant of PEP carboxylase for CO_2
g_s	2.5 mmol m^{-2} s^{-1}[c]	Bundle-sheath conductance to CO_2
g_o	0.047 g_s[d]	Bundle-sheath conductance to O_2
R_d	0.01* V_{cmax} (in Fig. 5 R_d = 0)	Leaf mitochondrial respiration
R_m	0.5 R_d	Mesophyll mitochondrial respiration
α	$0 < \alpha$ 1 (in Fig. 5 α = 0)	Fraction of PSII activity in the bundle sheath

[a] Jordan and Ogren, 1981. [b] Bauwe, 1986. [c] Brown and Byrd, 1993. [d] Farquhar 1983.

Model parameters used in Figure 5 are given in Table II.

ACKNOWLEDGMENTS

We thank Julie Styles and Sue Wood for the carbon isotope analysis of gas and dry matter samples. We thank Drs. John Evans and Katharina Siebke for helpful comments on the manuscript.

Received August 6, 1996; accepted November 4, 1996.
Copyright Clearance Center: 0032–0889/97/113/0469/09.

LITERATURE CITED

Bauwe H (1986) An efficient method for the determination of K_m values for HCO_3 of phosphoenolpyruvate carboxylase. Planta **169:** 356–360

Berry JA, Farquhar GD (1978) The CO_2 concentration function of C4 photosynthesis: a biochemical model. *In* D Hall, J Coombs, T Goodwin, eds, Proceedings of the 4th International Congress on Photosynthesis. Biochemical Society, London, pp 119–131

Bowman WD, Hubick KT, von Caemmerer S, Farquhar GD (1989) Short-term changes in leaf carbon isotope discrimination in salt- and water-stressed C_4 grasses. Plant Physiol **90:** 162–166

Brown RH (1978) A difference in N use efficiency in C_3 and C_4 plants and its implication in adaptation and evolution. Crop Sci **18:** 93–98

Brown RH, Byrd GT (1993) Estimation of bundle sheath cell conductance in C_4 species and O_2 insensitivity of photosynthesis. Plant Physiol **103:** 1183–1188

Butz ND, Sharkey TD (1989) Activity ratios of ribulose-1,5-bisphosphate carboxylase accurately reflect carbamylation ratios. Plant Physiol **89:** 735–739

Chitty JA, Furbank RT, Marshall JS, Chen Z, Taylor WC (1994) Genetic transformation of the C_4 plant *Flaveria bidentis*. Plant J **6:** 949–956

Collatz GJ, Ribas-Carbo M, Berry JA (1992) Coupled photosynthesis-stomatal model for leaves of C4 plants. Aust J Plant Physiol **19:** 519–538

Deleens E, Fehri A, Quieroz O (1983) Carbon isotope fractionation by plants using the C_4 pathway. Physiol Veg **21:** 897–905

Ehleringer J, Pearcy RW (1983) Variation in quantum yields for CO_2 uptake among C_3 and C_4 plants. Plant Physiol **73:** 555–559

Evans JR, Sharkey TD, Berry JA, Farquhar GD (1986) Carbon isotope discrimination measured concurrently with gas exchange to investigate CO_2 diffusion in leaves of higher plants. Aust J Plant Physiol **13:** 281–292

Evans JR, von Caemmerer S, Setchell BA, Hudson GS (1994) The relationship between CO_2 transfer conductance and leaf anatomy in transgenic tobacco with reduced content of Rubisco. Aust J Plant Physiol **21:** 475–495

Farquhar GD (1983) On the nature of carbon isotope discrimination in C_4 species. Aust J Plant Physiol **10:** 205–226

Farquhar GD, Ehleringer JR, Hubick RT (1989) Carbon isotope discrimination and photosynthesis. Annu Rev Plant Physiol Plant Mol Biol **40:** 503–537

Farquhar GD, von Caemmerer S, Berry JA (1980) A biochemical model of photosynthetic CO_2 assimilation in leaves of C_3 species. Planta **149:** 78–90

Furbank RT, Chitty JA, von Caemmerer S, Jenkins CLD (1996) Antisense RNA inhibition of *Rbc*S gene expression in the C_4 plant *Flaveria bidentis*. Plant Physiol **111:** 725–734

Furbank RT, Hatch MD (1987) Mechanism of C_4 photosynthesis. The size and composition of the inorganic carbon pool in bundle-sheath cells. Plant Physiol **85:** 958–964

Furbank RT, Jenkins CLD, Hatch MD (1990) C_4 photosynthesis: quantum requirements, C_4 acid overcycling and Q-cycle involvement. Aust J Plant Physiol **17:** 1–7

Furbank RT, Leegood RC (1984) Carbon metabolism and gas-exchange in leaves of *Zea mays* L. Interaction between the C_3 and C_4 pathways during photosynthetic induction. Planta **162:** 457–462

Hatch MD (1987) C_4 photosynthesis, a unique blend of modified biochemistry, anatomy and ultrastructure. Biochim Biophys Acta **895:** 81–106

Hatch MD, Agostino A, Jenkins CLD (1995) Measurement of the leakage of CO_2 from bundle sheath cells of leaves during C_4 photosynthesis. Plant Physiol **108:** 173–181

Hatch MD, Osmond CB (1976) Compartmentation and transport in C_4 photosynthesis. *In* CR Stocking, U Heber, eds, Transport in Plants. III. Intracellular Interactions and Transport Processes. Encyclopedia of Plant Physiology, New Series, Vol 3. Springer-Verlag, Berlin, pp 144–184

Henderson SA, von Caemmerer S, Farquhar GD (1992) Short-term measurements of carbon isotope discrimination in several C_4 species. Aust J Plant Physiol **19:** 263–285

Hewitt EJ, Smith TA (1975) Plant Mineral Nutrition. The English University Press, London

Hudson GS, Evans JR, von Caemmerer S, Arvidsson YBC, Andrews TJ (1992) Reduction of ribulose-bisphosphate carboxylase/oxygenase content by antisense RNA reduced photosynthesis in tobacco plants. Plant Physiol **98:** 294–302

Hunt ER, Weber JA, Gates DM (1985) Effects of nitrate application on *Amaranthus powellii* Wats. III. Optimal allocation of leaf nitrogen for photosynthesis and stomatal conductance. Plant Physiol **79:** 619–624

Jenkins CLD, Furbank RT, Hatch MD (1989) Inorganic carbon diffusion between C_4 mesophyll and bundle sheath cells. Plant Physiol **91:** 1356–1363

Jordan DB, Ogren WL (1981) Species variation in the specificity of ribulose carboxylase/oxygenase. Nature **291:** 513–515

Mate CJ, Hudson GS, von Caemmerer S, Evans JR, Andrews TJ (1993) Reduction of ribulose carboxylase activase levels in tobacco (*Nicotiana tabacum*) by antisense RNA reduces ribulose bisphosphate carboxylase carbamylation and impairs photosynthesis. Plant Physiol **102:** 1119–1128

O'Leary MH (1981) Carbon isotope fractionation in plants. Photochemistry **20:** 553–567

Peisker M (1982) The effect of CO_2 leakage from the bundle-sheath cells on carbon isotope composition. Photosynthetica **16:** 533–541

Raven JA (1977) Ribulose bisphosphate carboxylase activity in terrestrial plants: significance of O_2 and CO_2 diffusion. Curr Adv Plant Sci **9:** 579–590

Sage FR, Pearcy WR, Seemann JR (1987) The nitrogen use efficiency of C_3 and C_4 plants. III. Leaf nitrogen effects on the activity of carboxylating enzymes in *Chenopodium album* (L.) and *Amaranthus retroflexus* (L.). Plant Physiol **85:** 355–359

Sugiyama T, Hirayama Y (1983) Correlation of the activities of phosphoenolpyruvate carboxylase and pyruvate, orthophosphate dikinase with biomass in maize seedlings. Plant Cell Physiol **24:** 783–787

Usuda H (1984) Variations in the photosynthesis rate and activity of photosynthetic enzymes in maize leaf tissue of different ages. Plant Cell Physiol **25:** 1297–1301

Usuda H, Ku MSB, Edwards GE (1984) Rates of photosynthesis relative to activity of photosynthetic enzymes, chlorophyll and soluble protein content among ten C_4 species. Aust J Plant Physiol **11:** 509–517

von Caemmerer S, Evans JR (1991) Determination of the average partial pressure of CO_2 in chloroplasts from leaves of several C_3 plants. Aust J Plant Physiol **18:** 287–305

von Caemmerer S, Farquhar GD (1981) Some relationships between the biochemistry of photosynthesis and the gas exchange of leaves. Planta **153:** 376–387